

Radiation dose and image quality of CT fluoroscopy with partial exposure mode

Keisuke Takiguchi 

Atsushi Urikura 

Tsukasa Yoshida 

Yoshihiro Nakaya 

Masahiro Endo 

Takeshi Aramaki 

PURPOSE

The present study aimed to evaluate the scan technique of computed tomography (CT)-guided puncture procedures using partial exposure mode (PEM) on the radiation dose of the operator's hand and image quality.

METHODS

Radiation dose was evaluated using three types of scanning methods: one-shot scan (OS), OS with a bismuth shield added (OS_{Bismuth}), and a half-scan (i.e., PEM) capable of an adjustable exposure angle. Dose evaluation was performed using a torso phantom, while a circular phantom simulating the liver parenchyma and lesions was used for image quality evaluation. For each scanning method, four measurements were made to determine the radiation dose to the operator's hand and the dose distribution on the surface of the patient's torso; the output-dose profile was determined from five measurements. Image quality was evaluated in terms of contrast and contrast-to-noise ratio (CNR). Analysis of variance (ANOVA) or Friedman test were used for comparison between groups as appropriate. The post hoc tests were Tukey's honestly difference (HSD) test for parametric data or Wilcoxon signed rank test with Bonferroni correction for non-parametric data.

RESULTS

The PEM yielded a radiation dose to the operator's hand that was 84% (0.35 vs. 2.33 mGy) lower than that of the OS. The dose to the patient's torso was reduced by 35% and 68% for the OS_{Bismuth} and PEM, respectively, relative to that of the OS. Compared with the CNR of the other two scanning methods (OS, 2.9 ± 0.1 ; OS_{Bismuth} , 2.9 ± 0.1), the PEM increased the standard deviation and decreased the CNR (2.1 ± 0.04 , Tukey's HSD, $P < 0.001$ for all). Images acquired with PEM showed visibility equivalent to that of other scanning methods when window conditions were adjusted.

CONCLUSION

This study demonstrated that CT-guided puncture procedure using PEM effectively reduces the operator's exposure to radiation while minimizing image quality deterioration.

Currently, image-guided puncture procedures, such as computed tomography (CT)-guided puncture procedures, are widely used in interventional radiology (IR). CT fluoroscopy (CTF) was developed in the 1990s (1) and is used extensively for lung biopsy, radiofrequency ablation, abscess drainage, and lymph node biopsy (2–5). Most notably, CTF facilitates a safe puncture procedure; and the use of CT-guidance in fluoroscopy significantly shortens the examination time while reducing the radiation dose (6, 7).

The angio-CT system is a safe and accurate IR procedure. However, it presents a significant increase in radiation exposure compared with X-ray fluoroscopy-guided procedures. Even with CTF, the operator performs the puncture procedure near the CT gantry, which increases the risk of radiation exposure to the operator's fingers and lenses (7, 8).

The radiation exposure to the fingers of the operator is direct when performing CTF. Direct X-rays must be shielded to reduce the operator's exposure to radiation. As conventional CTF continuously emits X-rays, the consequent flux from the upper part of the gantry can only be shielded by protective equipment; the use of lead gloves or puncturing devices that reportedly reduce contact with direct X-rays (9, 10).

From the Radiation and Proton Therapy Center (K.T. [✉ k.takiguchi@scchr.jp](mailto:k.takiguchi@scchr.jp), T.Y.), Division of Diagnostic Radiology (A.U., Y.N., M.E.), Division of Interventional Radiology (T.A.), Shizuoka Cancer Center, Shizuoka, Japan.

Received 20 February 2019; revision requested 10 April 2019; last revision received 10 September 2019; accepted 03 November 2019.

Published online 27 May 2020.

DOI 10.5152/dir.2019.19091

You may cite this article as: Takiguchi K, Urikura A, Yoshida T, Nakaya Y, Endo M, Aramaki T. Radiation dose and image quality of CT fluoroscopy with partial exposure mode. *Diagn Interv Radiol* 2020; 26:333–338.

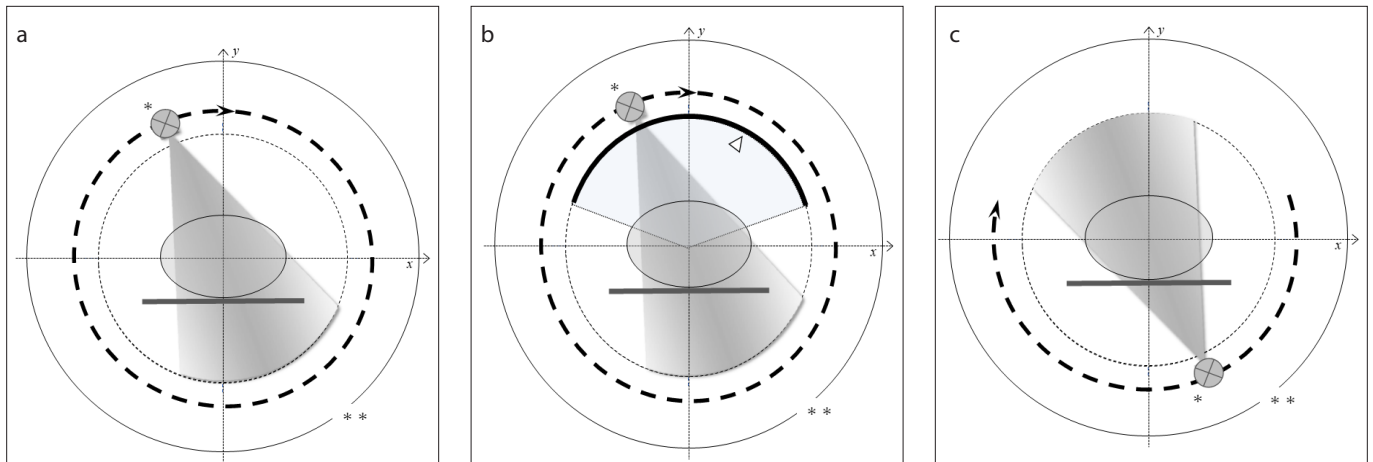


Figure 1. a–c. The three scanning methods used in the study. One-shot scan (OS) is a conventional one-rotation scan (a). $OS_{Bismuth}$ is OS with a bismuth shield (arrowhead) used to reduce X-rays from the upper portion of the gantry (b). A bismuth shield (1 mm thick, F & L Medical Products) was affixed to the inner side of the Mylar ring, from 10 o'clock to 2 o'clock positions. Partial exposure mode (PEM) is a half-scan in which an operator can arbitrarily determine the exposure angle (c). Single asterisk depicts the X-ray tube and double asterisks depicts the CT gantry.

The contemporary CTF adopts a different approach to reduce radiation exposure by incorporating technologic developments that reduce X-ray output from the upper part of the gantry (11, 12). Furthermore, an advanced angio-CT system (Infinix Celeve-i/Aquilion ONE VISION, Canon Medical Systems) uses a novel CTF technology (partial exposure mode; PEM) to apply half-scans, which precludes continuous X-ray irradiation. PEM is a half-scan in which the operator arbitrarily determines the center angle of the scan angle range ($180^\circ + \text{fan angle}$) for instant image acquisition at a constant scan time independent of the operator's experience. For more dynamic imaging, the operator presses the exposure switch in increments. Because the half-scan eliminates X-ray radiation from the upper part of the gantry, the operator's exposure to radiation during the puncture procedure is also significantly reduced.

Besides, since the center angle of the half-scan can be set arbitrarily, the radiation dose to radiation-susceptible organs such as the patient's ocular lenses and mammary glands is also reduced. However, the half-

scan of PEM is disadvantaged by a limited irradiation angle. Even though PEM can be performed with a significantly lower radiation dose compared with the conventional CTF, the use of lower radiation doses can result in an inferior image quality that interferes with the CT-guided puncture procedure.

To the best of our knowledge, studies on the relationship between radiation dose and image quality are lacking. This study aims to evaluate the radiation dose and image quality by using PEM in CT-guided puncture procedures and discusses the advantages and drawbacks of PEM.

We therefore measured how the radiation dose to the hand of the operator, surface dose to the patient's body torso, output dose distribution, and image quality of a CT-guided puncture procedure employing PEM compare with those achieved by more conventional scanning methods. The primary outcomes included radiation dose to the operators' hand, surface dose to the patients' torso, output dose distribution, and image quality of the CT-guided puncture procedure in PEM compared with more conventional scanning methods.

advanced angio-CT systems was used in this study to collect data for evaluating radiation doses and image quality. We used three scanning methods for data comparisons. The first method was the one-shot scan (OS), or a conventional, one-rotation CTF (Fig. 1a). This is the reference method to which the radiation dose and image quality of the PEM were compared. The second method was the one-shot scan with an attached bismuth shield ($OS_{Bismuth}$), which reduces X-ray irradiation above the gantry (Fig. 1b). The 1 mm thick bismuth shield (F & L Medical Products) was affixed to the inner side of the Mylar ring, spanning four clock hours from the 10 o'clock position to the 2 o'clock position. The third method was the PEM, which is a new scanning method that allows for a half-scan only (Fig. 1c). An operator can determine an arbitrary exposure angle via the scan console. In this study, we carried out the PEM evaluation from the 6 o'clock position. The scan parameters in all three methods were set to the following: tube voltage, 120 kVp; tube current, 50 mA; reconstructed image matrix, 512×512 ; reconstruction kernel, FC 13; slice thickness, 6 mm; field of view (FOV), 320 mm; rotation time, 0.5 s. The exposure time was 0.5 s for OS and $OS_{Bismuth}$, 0.32 s for PEM.

Radiation dose measurement

Fig. 2a shows the geometric layout for radiation dose measurement. The top of the torso phantom (Kyoto Kagaku) was set to the height of the center of rotation. To evaluate the dose to the operator's hands, we

Main points

- We report a technical improvement of angio-CT called partial exposure mode to reduce the radiation dose.
- Partial exposure mode reduces radiation exposure to the operator's hands.
- Partial exposure mode may yield visibility similar to conventional images, with setting adjustments.

Methods

The phantom imaging and radiation dose measurement was conducted according to the principles of the World Medical Association Declaration of Helsinki.

Data acquisition and scan parameters

An area-detector CT scanner (Aquilion ONE VISION Edition) installed in one of the

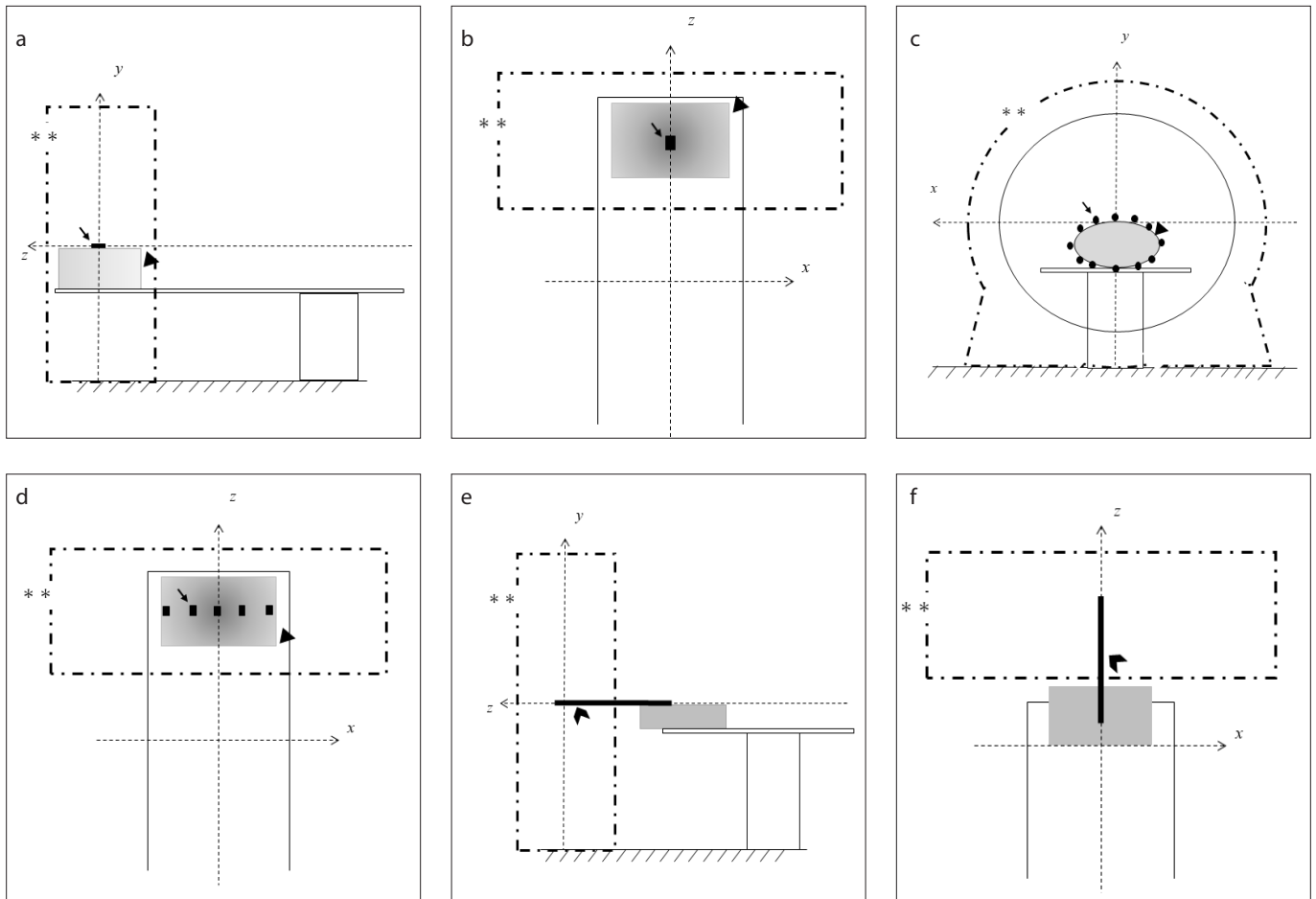


Figure 2. a–f. Layout for radiation dose measurement. Lateral view (a) and upper view (b) show a layout of the measurement point A, which simulates the position of the operator's finger. A glass dosimeter (arrow) was placed on the phantom (arrowhead). The phantom position was oriented downward, emulating a clinical condition such as a CT-guided puncture. Anterior view (c) and upper view (d) show the layout for measuring the patient's body-surface radiation dose. A glass dosimeter (arrow) was placed around the phantom (arrowhead) on the fan beam. The phantom position was the same as in (a) and (b). Lateral view (e) and upper view (f) show the layout for measuring the output-dose profile. A CT dose profiler (arrowhead, Piranha, RTI Electronics) was placed in the isocenter of the CT gantry. Single asterisk depicts X-ray tube and double asterisks depicts CT gantry.

placed a glass dosimeter on the upper side (point A) of the torso phantom. This placement was informed by the position of the fingers when the operator performed the puncture. We obtained four measurements for each CT scan.

A glass dosimeter was placed at 12 equally spaced points on the phantom as shown in Fig. 2b to obtain the dose distribution on the patient's body surface. Similar to Fig. 2a, four measurements were obtained for each CT scan. Also, the average radiation doses at five points (glass dosimeters) from 10 o'clock to 2 o'clock were calculated and compared for each scan. The glass dosimeter was annealed at 400°C for 30 min before each exposure and preheated at 70°C for 30 min after the scan was completed. The doses on the glass dosimeter were read using an FDG-1000 dose reader (AGC Techno Glass) (13, 14).

Measurement of the output-dose profile

The dose profiles were measured to evaluate the output-dose distribution of each scanning method. To obtain each profile, we used a wireless CT dose profiler device (Piranha, RTI Electronics) equipped with a small, 2×2×0.3 mm semiconductor detector designed for application to CT dosimetry (15). We placed the Piranha in the isocenter of the CT gantry, as shown in Fig. 2e. For display and storage, the dose profile data was stored on a laptop computer installed with Ocean software (RTI Electronics). We obtained five measurements for each CT scan.

Image quality

The phantom cross-section is shown in Fig. 3. To simulate the CT values of low-attenuation masses and abscesses in the liver parenchyma, a water-filled cylindrical rod with a CT value lower than that of the background

was enclosed in the cylindrical phantom. We used a 200 mm diameter cylindrical phantom filled with a 14.3% (w/v) sucrose solution for the background. This phantom adopted the same configuration as that shown in Fig. 2a. Circular regions of interest (ROI) with diameters of 20 mm and 30 mm were placed at the center of the phantom and in the background, respectively. First, the contrast was defined as the difference between the CT values of the central rod and the background. Second, as the indicator for image quality evaluation, the contrast-to-noise ratio (CNR) was calculated from equation (1).

$$\text{CNR} = \frac{|\text{ROI}_S - \text{ROI}_{BG}|}{\sqrt{\frac{1}{2}(\text{SD}_S^2 + \text{SD}_{BG}^2)}} \quad (1);$$

where ROI_S is the CT value (= 0 HU) of the central rod, ROI_{BG} is the CT value of the

background (≈ 50 HU), and SD_{BG} is the standard deviation (SD) of the CT value of ROI_{BG} . We determined the mean value of 10 measurements taken under each condition.

Statistical analysis

We compared the contrast and CNR obtained with each scanning mode. Repeated measures analysis of variance (ANOVA) or Friedman test was used for comparison between groups. The post hoc tests used were Tukey's honestly significant difference (HSD) test for parametric data or Wilcoxon

signed-rank test with Bonferroni correction for nonparametric data. $P < 0.05$ was considered statistically significant. All statistical analyses were performed using R software (version 3.2.3; R Project for Statistical Computing).

Results

The radiation doses of the OS, $OS_{Bismuth}$, and PEM to the operator's hands were 2.33 ± 0.2 , 1.40 ± 0.03 , and 0.35 ± 0.02 mGy, respectively. The OS exposed the operator's hands to the most radiation, while the $OS_{Bismuth}$ and PEM

irradiated doses 40% and 84% less than the OS, respectively.

Fig. 4 shows the radiation-dose distribution to the patient's body surface. Compared with the OS, the $OS_{Bismuth}$ reduced the mean radiation dose above the gantry by 35%, while the PEM reduced the dose at the same site by 68%.

Fig. 5 shows the output-dose profile of each scanning method. Although the starting angle of the X-ray irradiation for each scanning method was not fixed, the radiation dose of the OS increased twofold across certain ranges of angles. The radiation dose profile of the $OS_{Bismuth}$ decreased by 51% between 10 o'clock and 2 o'clock and, similar to the OS, featured a range of angles where its irradiation increased. The dose profile of PEM showed no X-ray irradiation above the gantry between the 10 o'clock and 2 o'clock positions.

Table shows the contrast and CNR for each scanning method. Data are presented as mean \pm SD. There was no significant difference in contrast between the scanning modes (repeated measures ANOVA, $P = 0.15$). There were significant differences in the CNR between the groups (repeated measures ANOVA, $P < 0.001$). The OS and $OS_{Bismuth}$ showed no significant difference (Tukey's HSD = 2.9 ± 0.1 vs. 2.9 ± 0.1 , respectively; $P = 0.33$). The CNR was significantly reduced in the PEM (2.1 ± 0.04) relative to OS (2.9 ± 0.1) and $OS_{Bismuth}$ (2.9 ± 0.1) (Tukey's HSD, $P < 0.001$ for all). Displayed on the scanner console, the value of $CTDI_{vol}$ was 2.7 mGy for OS and $OS_{Bismuth}$ and 1.7 mGy for PEM.

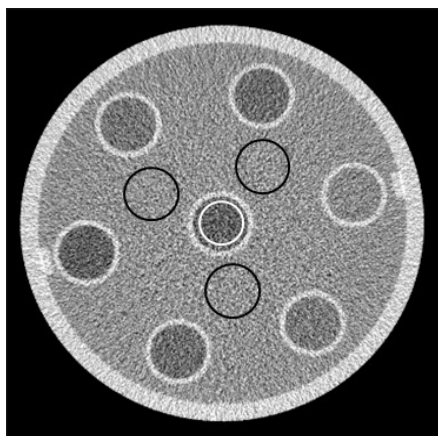


Figure 3. Region of interest (ROI) setting for image quality evaluation. The figure shows the phantom image acquired with CTF. ROI_{Ai} (white circle) is the circular ROI with a 20 mm diameter set at the rod in the phantom center, which simulates the low-attenuation lesion (CT value = 0 HU). ROI_{BG} (black circle) is the circular ROI with a 30 mm diameter set at three positions around the rod, which simulate the background liver parenchyma (CT value = 50 HU).

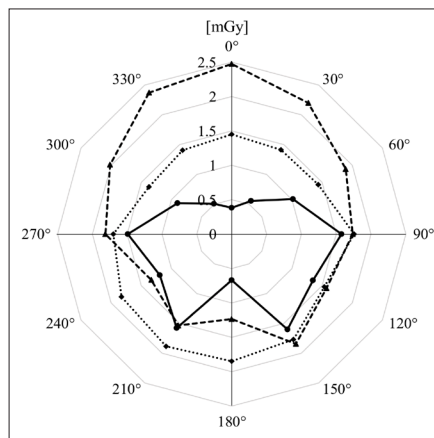


Figure 4. The patient's surface dose distribution using the three scanning modes. The figure shows the patient's surface dose obtained with each scanning mode (OS: triangle plots; $OS_{Bismuth}$: diamond plots; PEM: circle plots). The plots show an average of 10 measurements for each scanning mode. PEM significantly reduced the dose at the top of the gantry.

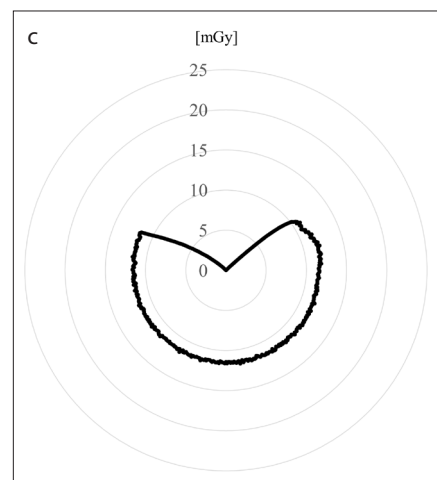
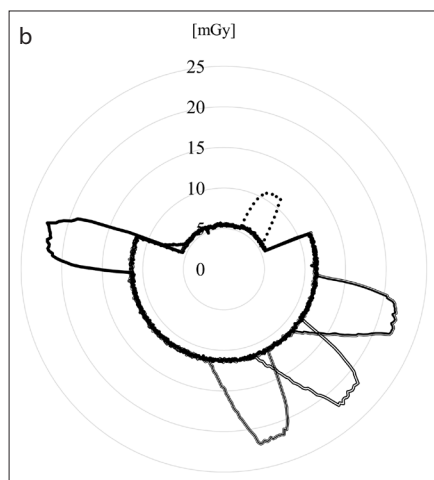
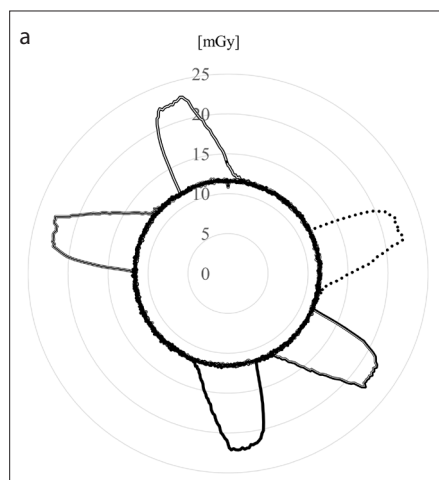


Figure 5. a–c. Output-dose profile of the three scanning methods. The figure shows the output-dose profile obtained with each scanning method. The plots show the superposition of each of the five measurements. Panels (a), (b), and (c) correspond to the output-dose profiles of OS, $OS_{Bismuth}$, and PEM, respectively. In panels (a) and (b), dose increased when exposure overlap associated with the fan beam angle occurred. Additionally, the dose increases were observed at an arbitrary position because the start position of the tube rotation was not fixed. The output-dose profile of the PEM, shown in panel (c), demonstrates a decrease in the dose above the gantry.

Table. Image quality parameters

Parameters	Imaging method			<i>P</i> (ANOVA) ^a	<i>P</i> (Tukey's HSD) ^b		
	PEM	OS	OS _{Bismuth}		PEM vs. OS	PEM vs. OS _{Bismuth}	OS vs. OS _{Bismuth}
Contrast [HU]	56.1±0.5	54.9±0.3	55.0±0.6	0.15	-	-	-
CNR	4.2±0.1	4.9±0.1	4.9±0.1	<0.001	<0.001	<0.001	0.34

All values are presented as mean ± SD; *P* < 0.05 is statistically significant.

PEM, partial exposure mode; OS, one-shot scan; ANOVA, analysis of variance; HSD, honestly significant test; HU, Hounsfield unit; CNR, contrast-to-noise ratio.

^aANOVA was used for comparison between three scanning modes.

^bCNR was compared by Tukey's HSD.

Discussion

The present study evaluated the radiation dose to the IR operator's hand, dose distribution on the surface of the patient's body, output-dose profile, and image quality yielded by three different scanning methods. In IR, CTF is often conducted with the subject oriented downward to allow for the puncture procedure. This arrangement places the operator's hands near the center of rotation. As the X-ray intensity at the center of rotation is relatively high due to the bow-tie filter mounted to optimize the intensity distribution of the CT X-ray flux (16, 17), the operator's hand is exposed to direct X-ray irradiation. Relative to the OS, we found that the OS_{Bismuth} and PEM reduced the radiation dose to the operator's hands; in particular, the irradiation of PEM at point A was reduced by approximately 84%. Point A was within the X-ray irradiation field and was directly exposed to the X-ray, but by limiting the exposure range of PEM to the side of the bed (below the gantry), we precluded X-ray emission above the gantry. Relative to the OS, the radiation dose from OS_{Bismuth} showed a 40% reduction. This result agreed with the prior bismuth shield studies (18, 19). Although this scanning method is inferior to PEM in terms of the radiation to which it exposes the operator, it only requires the addition of a bismuth shield to the existing CT apparatus. Since the bismuth shield is an inexpensive, lightweight, easy to produce and handle latex sheet, it is a simple solution to significantly reduce the radiation dose. Also, since the bismuth shield is affixed inside the Mylar ring, it does not affect the conventional IR procedure.

The analysis of the radiation dose distribution on the patient's body surface revealed a relationship between the scanning method and the surface dose. The OS radiation dose exhibited a lower value below the gantry than above it. As the output

dose is constant, the dose reduction below the gantry may reflect X-ray absorption by the surface on which the patient lays. Using the OS_{Bismuth}, the radiation dose above the gantry was reduced up to 42% relative to the OS. Moreover, the mean dose in the 10 o'clock to 2 o'clock positions were reduced by 35% with the bismuth shield, thus demonstrating its efficacy in reducing radiation doses above the gantry. The PEM exhibited a low radiation dose distribution above the gantry and was effective in attenuating the radiation dose to the patients.

To elucidate the output radiation dose distribution for each scanning method, we measured the output dose profiles. OS and OS_{Bismuth} exhibited dose levels that increased by approximately two-fold across a specific range of angles. Generally, in the full scan, X-rays are emitted 360° including the fan angle; and hence the dose levels tend to escalate across the fan angle due to double irradiation in this region. Besides, we found that the OS and OS_{Bismuth} varied in their radiation commencement position. If the fan angle is situated above the gantry, the operator's exposure to radiation increases; hence, the observed increase in radiation dose levels even with the application of the bismuth shield. Although it is possible to reduce the radiation dose by using a bismuth shield, it is not possible to avoid the influence of the fan angle in a full scan. However, the half-scan of the PEM precludes the possibility of double exposure by the fan angle. Furthermore, since it is possible for the operator to determine the scan range arbitrarily, the PEM lowers the radiation exposure to the operator and patient. The present study further compared the image quality between the three screening methods using a cylindrical phantom. The CNR of PEM decreased significantly relative to the oth-

er two scanning methods. The exposure time of PEM was shorter than that of the other scanning methods, which increased the image's SD. The decrease in CNR may diminish the ability of PEM to detect tumors. Even though the image's SD and CNR are significantly affected by PEM, the observed difference was minor, and it was possible to obtain an approximate visual impression by adjusting the PEM's window condition.

In recent years, the dose-reduction technology implemented by diagnostic CT in CTF has become applicable to new devices (20); and PEM is an example of such innovation with good potential to reduce the radiation dose to the operator.

This study is subject to several limitations. Since the phantom did not include structures such as bones or intestinal tracts, our analysis did not account for the noise or artifacts caused by such surrounding structures. Also, we did not use a large phantom that could possibly attenuate radiation by absorption. Neither did we investigate the influence of streak artifacts on the image caused by the puncture needle during the puncture procedure. Finally, this study only investigated a single vendor's CT systems, i.e., we did not evaluate other devices. We recommend considering the above factors in future studies.

In conclusion, the radiation doses and image qualities of three different scanning methods were evaluated to reduce the operators' radiation dose during CT-guided puncture procedures. The dose reduction achieved by the PEM was superior to that of the OS with and without a bismuth shield. Although the PEM affected the image SD and resulted in a slight decrease in the CNR, adjustment of the window setting can compensate for such deficiencies. The present study demonstrates that PEM is useful in reducing irradiation to the operator's hands and the patient's body surface during CT-guided puncture procedures.

Conflict of interest disclosure

The authors declared no conflicts of interest.

References

1. Katada K, Kato R, Anno H, et al. Guidance with real-time CT fluoroscopy: early clinical experience. *Radiology* 1996; 200:851–856. [\[Crossref\]](#)
2. Kim GR, Hur J, Lee SM, et al. CT fluoroscopy-guided lung biopsy versus conventional CT-guided lung biopsy: a prospective controlled study to assess radiation doses and diagnostic performance. *Eur Radiol* 2011; 21:232–239. [\[Crossref\]](#)
3. Daly B, Krebs TL, Wong-You-Cheong JJ, Wang SS. Percutaneous abdominal and pelvic interventional procedures using CT fluoroscopy guidance. *AJR Am J Roentgenol* 1999; 173:637–644. [\[Crossref\]](#)
4. Zech CJ, Helmberger T, Wichmann MW, Holzknecht N, Diebold J, Reiser MF. Large core biopsy of the pancreas under CT fluoroscopy control: results and complications. *J Comput Assist Tomogr* 2002; 26:743–749. [\[Crossref\]](#)
5. Yang K, Ganguli S, DeLorenzo MC, Zheng H, Li X, Liu B. Procedure-specific CT dose and utilization factors for CT-guided interventional procedures. *Radiology* 2018; 172945. [\[Crossref\]](#)
6. Gianfelice D, Lepanto L, Perreault P, Chartrand-Lefebvre C, Milete PC. Value of CT fluoroscopy for percutaneous biopsy procedures. *J Vasc Interv Radiol* 2000; 11:879–884. [\[Crossref\]](#)
7. Carlson SK, Bender CE, Classic KL, et al. Benefits and safety of CT fluoroscopy in interventional radiologic procedures. *Radiology* 2001; 219:515–520. [\[Crossref\]](#)
8. Silverman SG, Tuncali K, Adams DF, Nawfel RD, Zou KH, Judy PF. CT fluoroscopy-guided abdominal interventions: techniques, results, and radiation exposure. *Radiology* 1999; 212:673–681. [\[Crossref\]](#)
9. Kato R, Katada K, Anno H, Suzuki S, Ida Y, Koga S. Radiation dosimetry at CT fluoroscopy: physician's hand dose and development of needle holders. *Radiology* 1996; 201:576–578. [\[Crossref\]](#)
10. Sarmento S, Pereira JS, Sousa MJ, et al. The use of needle holders in CTF guided biopsies as a dose reduction tool. *J Appl Clin Med Phys* 2018; 19:250–258. [\[Crossref\]](#)
11. Hohl C, Suess C, Wildberger JE, et al. Dose reduction during CT fluoroscopy: phantom study of angular beam modulation. *Radiology* 2008; 246:519–525. [\[Crossref\]](#)
12. Teles P, Nikodemová D, Bakhanova E, et al. A review of radiation protection requirements and dose estimation for staff and patients in CT fluoroscopy. *Radiat Prot Dosimetry* 2017; 174:518–534. [\[Crossref\]](#)
13. Kawasaki T, Fujii K, Akahane K. Estimation of organ and effective doses for neonate and infant diagnostic cardiac catheterizations. *AJR Am J Roentgenol* 2015; 205:599–603. [\[Crossref\]](#)
14. Nishizawa K, Moritake T, Matsumaru Y, Tsuboi K, Iwaki K. Dose measurement for patients and physicians using a glass dosimeter during endovascular treatment for brain disease. *Radiat Prot Dosimetry* 2003; 107:247–252. [\[Crossref\]](#)
15. Matsubara K, Takata T, Kobayashi M, Kobayashi S, Koshida K, Gabata T. Tube current modulation between single- and dual-energy CT with a second generation dual-source scanner: radiation dose and image quality. *AJR Am J Roentgenol* 2016; 207:354–361. [\[Crossref\]](#)
16. Toth T, Ge Z, Daly MP. The influence of patient centering on CT dose and image noise. *Med Phys* 2007; 34:3093–3101. [\[Crossref\]](#)
17. Funama Y, Taguchi K, Awai K, Sakabe D, Shimamura M, Yamashita Y. Image noise and radiation dose using an automatic tube current modulation technique at 64-detector computed tomography: effect of off-center patient position, bowtie filter type, and scan projection radiograph. *J Comput Assist Tomogr* 2009; 33:973–977. [\[Crossref\]](#)
18. Wang J, Duan X, Christner JA, Leng S, Yu L, McCollough CH. Radiation dose reduction to the breast in thoracic CT: Comparison of bismuth shielding, organ-based tube current modulation, and use of a globally decreased tube current. *Med Phys* 2011; 38:6084–6092. [\[Crossref\]](#)
19. Vollmar SV, Kalender WA. Reduction of dose to the female breast in thoracic CT: a comparison of standard-protocol, bismuth-shielded, partial and tube-current-modulated CT examinations. *Eur Radiol* 2008; 18:1674–1682. [\[Crossref\]](#)
20. Grosser OS, Wybranski C, Kupitz D, et al. Improvement of image quality and dose management in CT fluoroscopy by iterative 3D image reconstruction. *Eur Radiol* 2017; 27:3625–3634. [\[Crossref\]](#)